Asymmetric gain-saturated spectrum in fiber optical parametric amplifiers

Zohreh Lali-Dastjerdi,* Karsten Rottwitt, Michael Galili, and Christophe Peucheret

DTU Fotonik, Department of Photonics Engineering, Technical University of Denmark, DK-2800 Kgs. Lyngby, Denmark

*zoda@fotonik.dtu.dk

Abstract: We demonstrate experimentally and numerically an unexpected spectral asymmetry in the saturated-gain spectrum of single-pump fiber optical parametric amplifiers. The interaction between higher-order four-wave mixing products and dispersive waves radiated as an effect of third-order dispersion influences the energy transfer to the signal, depending on its detuning with respect to the pump, and breaks the symmetry of the gain expected from phase-matching considerations in unsaturated amplifiers. The asymmetry feature of the saturated spectrum is shown to particularly depend on the dispersion characteristics of the amplifier and shows local maxima for specific dispersion values.

OCIS codes: (190.4380) Four-wave mixing; (190.4410) Parametric processes; (190.4970) Parametric oscillators and amplifiers.

References and links

1. K. Inoue, "Optical level equalisation based on gain saturation in fibre optical parametric amplifier," Electron. Lett. **36**(12), 1016–1018 (2000).
2. C. Peucheret, M. Lorenzen, J. Seoane, D. Noordegraaf, C. V. Nielsen, L. Grüner-Nielsen, and K. Rottwitt, "Amplitude regeneration of RZ-DPSK signals in single-pump fiber-optic parametric amplifiers," IEEE Photon. Technol. Lett. **21**(13), 872–874 (2009).
3. A. Vedadi, A. M. Ariaei, M. M. Jadidi, and J. A. Salehi, "Theoretical study of high repetition rate short pulse generation with fiber optical parametric amplification," J. Lightwave Technol. **30**(9), 1263–1268 (2012).
4. K. Inoue and T. Mukai, "Experimental study of noise characteristics of a gain-saturated fiber optical parametric amplifier," J. Lightwave Technol. **20**(6), 969–974 (2002).
5. M. E. Marhic, *Fiber optical parametric amplifiers, oscillators and related devices* (Cambridge University Press, 2008), Chap. 5.
6. A. S. Y. Hsieh, G. K. L. Wong, S. G. Murdoch, S. Coen, F. Vanholsbeeck, R. Leonhardt, and J. D. Harvey, "Combined effect of Raman and parametric gain on single-pump parametric amplifiers," Opt. Express **15**(13), 8104–8114 (2007).
7. P. Kylemark, H. Sunnerud, M. Karlsson, and P. A. Andrekson, "Semi-analytical saturation theory of fiber optical parametric amplifiers," J. Lightwave Technol. **24**(9), 3471–3479 (2006).
8. K. Inoue and T. Mukai, "Signal wavelength dependence of gain saturation in a fiber optical parametric amplifier," Opt. Lett. **26**(1), 10–12 (2001).
9. N. Akhmediev and M. Karlsson, "Cherenkov radiation emitted by solitons in optical fibers," Phys. Rev. A **51**(3), 2602–2607 (1995).
10. A. K. Abeeluck and C. Headley, "Continuous-wave pumping in the anomalous- and normal-dispersion regimes of nonlinear fibers for supercontinuum generation," Opt. Lett. **30**(1), 61–63 (2005).
11. M. Droques, B. Barviau, A. Kudlinski, M. Taki, A. Boucon, T. Sylvestre, and A. Mussot, "Symmetry-breaking dynamics of the modulational instability spectrum," Opt. Lett. **36**(8), 1359–1361 (2011).
12. G. P. Agrawal, *Nonlinear Fiber Optics* 3rd ed. (Academic Press, 2006), Chap. 2 and 12.
13. K. Inoue and T. Mukai, "Spectral hole in the amplified spontaneous emission spectrum of a fiber optical parametric amplifier," Opt. Lett. **26**(12), 869–871 (2001).

1. Introduction

Optical parametric amplification based on four-wave mixing (FWM) and relying on the ultrafast third order nonlinearity of glass fibers is commonly used for all-optical signal processing, such as pulse generation, frequency conversion, amplitude regeneration etc [1–3]. The fast gain response of saturated fiber optical parametric amplifiers (FOPAs) enables the reduction of the intensity fluctuations of the input signal [2,4]. Such an application

#167424 - $15.00 USD Received 1 May 2012; revised 18 Jun 2012; accepted 19 Jun 2012; published 26 Jun 2012

necessitates the amplifier to operate in its saturated regime and therefore accentuates the need for proper characterization of the saturated gain spectra of FOPAs. Single-pump FOPAs working in the linear gain regime have only one dominant FWM product (idler), which is symmetrically located with respect to the pump frequency. In this case, the gain spectrum is symmetric with two gain peaks corresponding to two phase-matched signal frequencies around the pump. The symmetric feature of the unsaturated gain spectrum originates from the fact that the linear phase mismatch factor, $\Delta\beta$, depends only on even-order dispersion as well as on the even powers of the pump-signal frequency separation [5]. Some spectral asymmetry may however be observed for wideband unsaturated FOPAs as a result of stimulated Raman scattering [6]. In the nonlinear gain regime, the saturated gain spectrum remains symmetric as long as the higher-order FWM products (HFPs – FWM products other than the idler) do not grow significantly. However, under strong saturation conditions, the power of some of the HFPs may reach or even exceed the signal power and therefore those products can no longer be ignored in the analysis of the gain spectrum. The behavior of the gain spectrum of FOPAs in the nonlinear regime (i.e. under gain saturation) has been studied in a few papers [7,8], whereas in most reported applications using FOPAs in the saturation regime, only some specific wavelengths within the gain spectrum have been selected for operation. So far the existence of a gain difference between the two sides of the gain spectrum of single-pump FOPAs in saturation has neither been studied nor analyzed.

This paper reports an experimental observation of the asymmetry of the gain spectrum of single-pump FOPAs under strong saturation for the first time. The possible original physical mechanism leading to this new and different gain asymmetry is also clarified in terms of interaction between the first or second HFPs (1HFP or 2HFP) on the anti-Stokes side of the gain spectrum and emitted dispersive waves (DWs) shed by third-order dispersion (TOD). Numerical simulations verify the experimental results and show that the asymmetry feature depends on the dispersion terms of the amplifier.

2. Experimental observation

The effect discussed in this paper was first observed experimentally. The experimental setup is represented in Fig. 1(a). The pump signal originates from a continuous wave (CW) laser at λ_P = 1557.5 nm that is phase modulated using a 10-Gb/s 2^7-1 pseudorandom binary sequence (PRBS) to suppress stimulated Brillouin scattering, amplified by an erbium-doped fiber amplifier (EDFA) and filtered by a 1-nm bandwidth optical band pass filter (OBPF) to reduce the produced amplified spontaneous emission (ASE) noise.

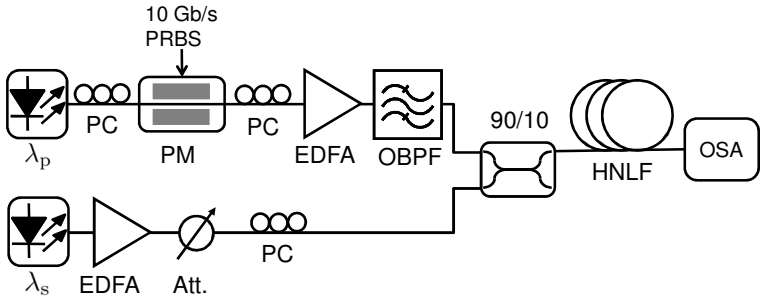

Fig. 1. Experimental setup for FOPA gain characterization.

#167424 - $15.00 USD Received 1 May 2012; revised 18 Jun 2012; accepted 19 Jun 2012; published 26 Jun 2012

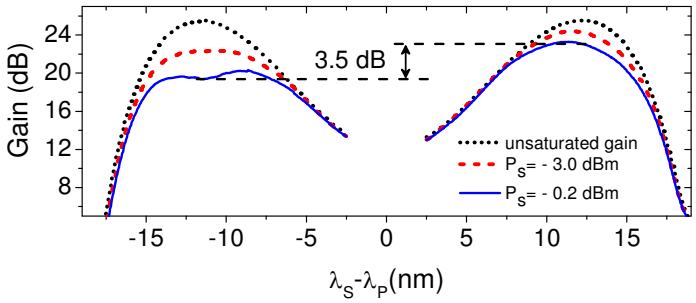

Fig. 2. Experimental signal gain spectra for different signal input powers.

A tunable laser source provides the signal, which is amplified by a flat-gain EDFA in the range of 1538 nm to 1575 nm and swept in wavelength. The input signal power is controlled by a variable attenuator (Att.). A 10/90% coupler combines the pump and signal, whose states of polarization are optimized with polarization controllers (PCs), into a 500-m long highly nonlinear fiber (HNLF) with zero-dispersion wavelength (ZDW) at $\lambda_0 = 1550.4$ nm, nonlinear coefficient of 10.7 $W^{-1}\cdot km^{-1}$, dispersion slope of 0.0185 ps/($nm^2\cdot$km), and attenuation of 0.7 dB/km. The pump power at the HNLF input is 28.6 dBm. The gain spectra are measured using an optical spectrum analyzer (OSA).

The experimentally measured signal gain spectra for unsaturated gain and signal input powers (P_S) of −3 dBm (modest saturation) and −0.2 dBm (strong saturation) are shown in Fig. 2. The experimental unsaturated gain spectrum is symmetric and has 25.4-dB gain at 1546 nm (anti-Stokes side) and 1570 nm (Stokes side). Clearly, one can see that the maximum gain drops differently at the two lobes of the spectrum when the gain enters saturation. The measured gain differences between the wavelengths corresponding to the maximum unsaturated gain are 1.9 dB and 3.5 dB when P_S is −3 dBm and −0.2 dBm, respectively.

3. Interplay of HFPs and dispersive waves

To understand the physical mechanism behind this unexpected gain asymmetry, the interaction between all the waves, present at the input of the amplifier as well as generated during propagating through the HNLF, is considered in both time and frequency domains. In FOPAs, an increase of the signal input power results in a growth of the FWM products. Figure 3(a) represents the nomenclature of the FWM products used throughout this work. The pump P and signal S generate an idler I. In the single-pump FOPAs considered here, HFPs (corresponding to FWM products other than the idler) are generated on an angular frequency grid $\Delta\omega_{PS} = |\omega_P - \omega_S|$. The n^{th} order HFP, noted nHFP, is at angular frequency $\omega_n = m\omega_S - (m-1)\omega_P$ on the signal side when $n = m-1$ (for integer $m \geq 2$), or on the idler side when $n = m + 1$ (for integer $m \leq -2$). In the time domain, the total (pump, signal, idler and HFPs) power appears as oscillations that transform into a train of short pulses when the number and power of the HFPs increase. Therefore, as the amplifier enters the saturation regime and short pulses are formed, higher order dispersion, and more specifically TOD, affect considerably the dynamic of the propagating waves. Since the pump is located in the anomalous dispersion region of the fiber, the short pulses are perturbed in the presence of TOD and emit DWs to become stable as fundamental solitons [9]. DWs are radiated at the anti-Stokes side of the spectrum in the normal dispersion region of the fiber when the phase matching condition between them and fundamental solitons is fulfilled. Similar considerations have been introduced for the interpretation of CW pumping in supercontinuum generation [10] and of symmetry-breaking of modulation instability spectra [11]. Assuming that dispersion orders higher than TOD can be neglected, the generated DWs are separated in frequency from the pump by $\Delta\omega_{DW}$ such that

$$\beta_3 \Delta\omega_{DW}^3 + 3\beta_2 \Delta\omega_{DW}^2 - 3\gamma P_P = 0, \qquad (1)$$

#167424 - $15.00 USD Received 1 May 2012; revised 18 Jun 2012; accepted 19 Jun 2012; published 26 Jun 2012

where β_2 and β_3 are the second-order dispersion (SOD) and TOD, respectively, P_P is the pump power and γ is the nonlinear coefficient [12]. Energy transfer to shorter wavelengths as DWs disturbs the symmetric FWM efficiency between the two sides of the gain spectrum. If the condition $\Delta\omega_{DW} = (n + 1)\Delta\omega_{PS}$ is satisfied, where n is an integer $n \geq 1$ and $\Delta\omega_{PS}$ is the pump-signal angular frequency separation, the DWs will overlap at the anti-Stokes side with the signal (when $\lambda_S < \lambda_P$) or idler (when $\lambda_S > \lambda_P$) for $n = 0$, the first order HFP for $n = 1$ (1HFP when $\lambda_S < \lambda_P$ or −1HFP when $\lambda_S > \lambda_P$) and so on.

Frequency matching between the generated DWs and HFPs for $|n| \geq 1$ reduces the energy transfer to the wavelength at $n = 0$ corresponding to the signal (idler) when $\lambda_S < \lambda_P$ ($\lambda_S > \lambda_P$), hence reducing the gain or conversion efficiency at the anti-Stokes side.

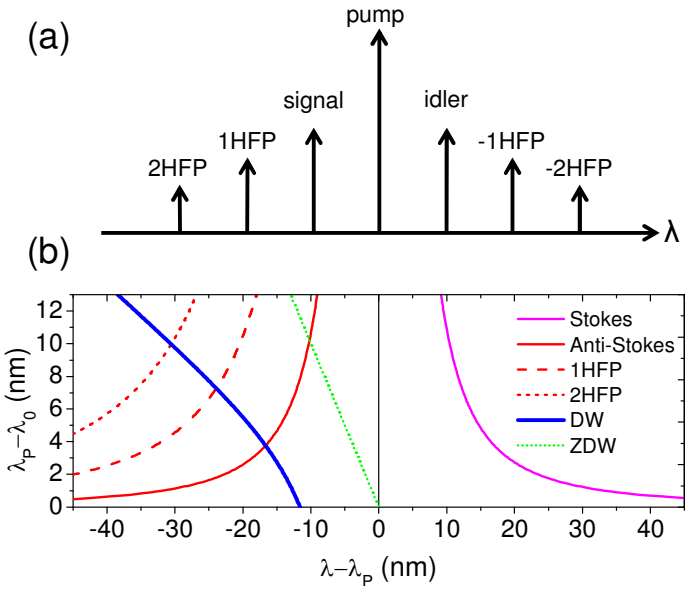

Fig. 3. (a) Nomenclature of the FWM products (a). (b) Wavelength positions of the maximum unsaturated gain at the Stokes and anti-Stokes sides of the pump, corresponding 1HFPs, 2HFPs, as well as DWs for different values of the detuning between the pump and the zero-dispersion wavelength $\Delta\lambda_{P0}$.

The wavelengths of the maximum unsaturated gain at the Stokes and anti-Stokes sides of the pump, corresponding 1HFPs and 2HFPs, and DWs are displayed in Fig. 3(b) as a function of the separation between the zero-dispersion and the pump wavelengths ($\Delta\lambda_{P0} = \lambda_P - \lambda_0$). As it can be seen, the wavelengths of the generated DWs overlap with the signal or the HFPs when $\Delta\lambda_{P0}$ is between 3 and 10 nm. In the experiment reported in Sect. 2, $\Delta\lambda_{P0} = 7.1$ nm, for which it can be seen from Fig. 3(b) that the 1HFP almost overlaps with the DWs, which leads to energy transfer to the 1HFP, which in turn reduces the signal gain at the anti-stokes side of the spectrum.

The growth of the ± 1HFP is well confirmed in Fig. 4, which shows the experimental output power of the pump, signal, idler and ± 1HFPs as a function of the signal input power for signals at 1546 nm and 1570 nm, corresponding to wavelengths of maximum unsaturated gain. For low signal input powers, the signal and idler waves grow identically, but for input powers above −5 dBm, the wave (signal or idler) located on the Stokes side gains more power as a result of the energy transfer to the first order HFP (1HFP for $\lambda_S = 1546$ nm or −1HFP for $\lambda_S = 1570$ nm) coinciding with the DWs on the anti-Stokes side. The steep power growth of the first order HFP on the anti-Stokes side is also clearly observed.

#167424 - $15.00 USD Received 1 May 2012; revised 18 Jun 2012; accepted 19 Jun 2012; published 26 Jun 2012

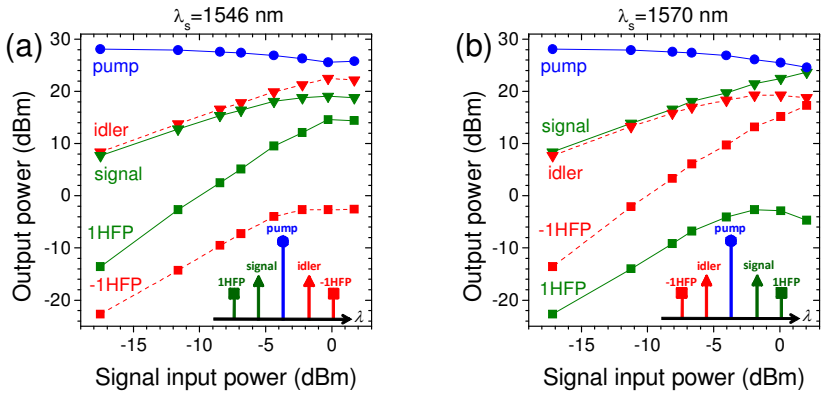

Fig. 4. Experimentally measured output power of the pump, signal, idler and ± 1HFPs for signal wavelengths equal to: (a) λ_s = 1546 nm (b) λ_s = 1570 nm.

4. Numerical simulations

The understanding of the interaction between the HFPs and generated DWs in strong saturation regime is confirmed in this section by simulations where different values of SOD and TOD have been examined. Simulations are carried out in order to support the proposed mechanism leading to different energy transfers to the waves at the two sides of the saturated gain spectrum. In this section, the gain spectrum of the amplifier implemented experimentally is first simulated. The simulations are then expanded in order to investigate the impact of SOD and TOD on the signal gain or idler conversion efficiency in the linear and nonlinear regimes.

The gain spectra are simulated by numerically solving the generalized nonlinear Schrödinger equation (NLSE) using the split-step Fourier method [12]. The NLSE used in this work takes the form

$$\frac{\partial A}{\partial z}+\frac{\alpha}{2}A+\frac{i}{2}\beta_2\frac{\partial^2 A}{\partial t^2}-\frac{1}{6}\beta_3\frac{\partial^3 A}{\partial t^3}=i\gamma|A|^2 A. \tag{2}$$

The initial complex envelop is the sum of those of the CW pump and signal

$$A(0,t)=\sqrt{P_P(0)}\exp(-i\omega_P t)+\sqrt{P_S(0)}\exp(-i\omega_S t), \tag{3}$$

where the angular frequencies are expressed relatively to the reference frequency used for baseband transformation. This approach is suitable for the problem under study since it enables to account for all the waves created through all the FWM processes. This is in contrast with the resolution of a system of coupled equations (one for each wave) which limits beforehand the number of waves taken into account and therefore may not be accurate in deep saturation conditions where a potentially large number of HFPs are involved.

The calculated gain spectra are shown in Fig. 5 for parameters identical to those of the experiment, as well as under stronger saturation with a signal input power of 1 dBm. The solid gain curves have been calculated according to Eq. (1) without taking SRS into account in the simulations. The simulation results are in very good agreement with the experiment. The gain differences between the two wavelengths corresponding to the maximum unsaturated gain are 2.1 dB, 3.7 dB and 4.7 dB when the signal input power is –3 dBm, –0.2 dBm, and 1 dBm, respectively. The small discrepancies observed between the simulated and measured gain spectra are believed to be due to the limited accuracy in the determination of the exact dispersive properties of the fiber used in the experiment and their longitudinal variations and to polarization effects.

#167424 - $15.00 USD Received 1 May 2012; revised 18 Jun 2012; accepted 19 Jun 2012; published 26 Jun 2012

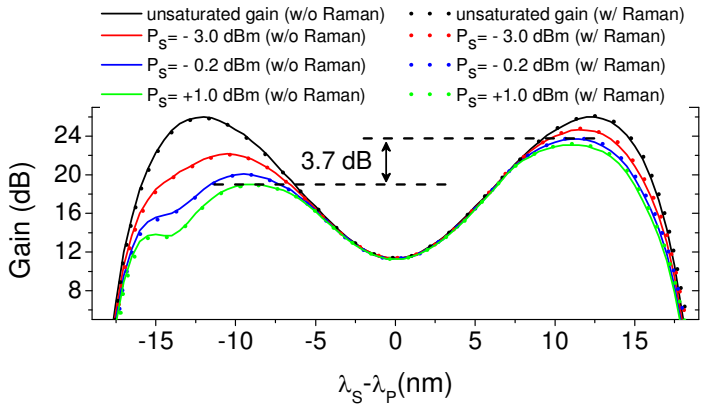

Fig. 5. Signal gain spectra simulated for different signal input powers with and without taking SRS into account.

The FOPA under investigation has a rather limited bandwidth, with a maximum unsaturated gain offset from the pump wavelength by 12 nm. Therefore one would not expect SRS, with a gain peak at about 100 nm above the pump wavelength, to significantly affect the gain spectrum and result in gain asymmetry for such a narrow bandwidth FOPA. This is confirmed when examining both measured and calculated unsaturated gain spectra in Fig. 2 and Fig. 5, respectively, which appear symmetric. In order to further confirm that the observed asymmetry is not related to SRS, the gain calculations are repeated by taking SRS into account. In these simulations, the SRS effect is modeled conventionally by adding a delayed nonlinear response term to Eq. (2) corresponding to a single-Lorentzian approximation of the Raman gain [12]. The corresponding FOPA gain spectra are also represented in Fig. 5. It clearly appears that SRS has very little impact on the calculated gain spectra and therefore does not contribute significantly to the reported spectral asymmetry.

As the wavelengths of the DWs, hence $\Delta\omega_{DW}$, depend on both SOD and TOD, their overlaps with the HFPs can be tuned by adjusting either the SOD or TOD of the fibre. Modification of the SOD can modify both the wavelength of the phase-matched signal and that of the DWs, while variations of TOD has an impact only on the wavelength of the DWs as the phase-matched signal wavelength depends only on SOD. Here we investigate the effect of both dispersion terms.

4.1 Impact of SOD

The bandwidth of FOPAs depends on the fulfillment of the phase-matching condition, which under the assumption that dispersive effects higher than β_3 can be neglected, and in the unsaturated regime (i.e. the pump power dominates over the power of the signal and idler), is expressed as

$$\Delta\beta + 2\gamma P_P = \beta_2(\omega_P)\Delta\omega_{PS}^2 + 2\gamma P_P = 0, \tag{4}$$

where $\Delta\beta$ is the linear phase mismatch parameter. In what follows, the bandwidth of the FOPA is defined as the frequency separation between the two phase-matched signal wavelengths, i.e.

$$2\Delta\omega_{PS} = 2\sqrt{\frac{2\gamma P_P}{|\beta_2(\omega_P)|}}. \tag{5}$$

The amplifier bandwidth can be tuned by tuning the pump wavelength, hence changing the value of SOD at this wavelength. The wavelength of the radiated DWs in deep saturation can be subsequently tuned as well. Consequently, the signal at the maximum unsaturated gain or corresponding HFPs on the short wavelength side of the spectrum can be made to overlap

#167424 - $15.00 USD Received 1 May 2012; revised 18 Jun 2012; accepted 19 Jun 2012; published 26 Jun 2012

with DWs, as can be seen in Fig. 3(b), depending on the dispersion value at the pump wavelength or, equivalently, $\Delta\lambda_{P0}$. In order to evaluate the effect of amplifier bandwidth, or equivalently SOD, on the saturated gain, the signal gain and idler conversion efficiency spectra are simulated for three bandwidths obtained with three different values of $\Delta\lambda_{P0}$ corresponding to emitted DWs overlapping with the phase-matched signal, 1HFP and 2HFP, respectively. Figure 6(a)-(c) show the saturated signal gain and idler conversion efficiency spectra and Fig. 6(d)-(f) show the output spectra for signals tuned to the maximum unsaturated gain on the short wavelength side of the spectrum. The signal input power is −0.2 dBm and all other parameters are the same as those in the experiment. The idler conversion efficiency spectra are mirror images of the signal spectra as they are plotted as a function of the signal-pump wavelength separation. The significant growth of the 1HFP and 2HFP are obvious in Fig. 6(b),(e) and Fig. 6(c),(f), respectively, when the HFPs are resonant with the emitted DWs. The saturated gain difference between the two sides of the spectrum is 0.2 dB, 5.1 dB and 4.4 dB for the broad, relatively narrow and narrow-band amplifiers in Fig. 6(a)-(c), respectively. A movie (Media 1) illustrating the temporal and spectral evolution of the total output power with $\Delta\lambda_{P0}$ (or equivalently $\beta_2(\omega_P)$) can be seen online. The simulations presented in the movie confirm well the growth of HFPs when they are close to DW wavelengths depicted by dashed blue line in the movie.

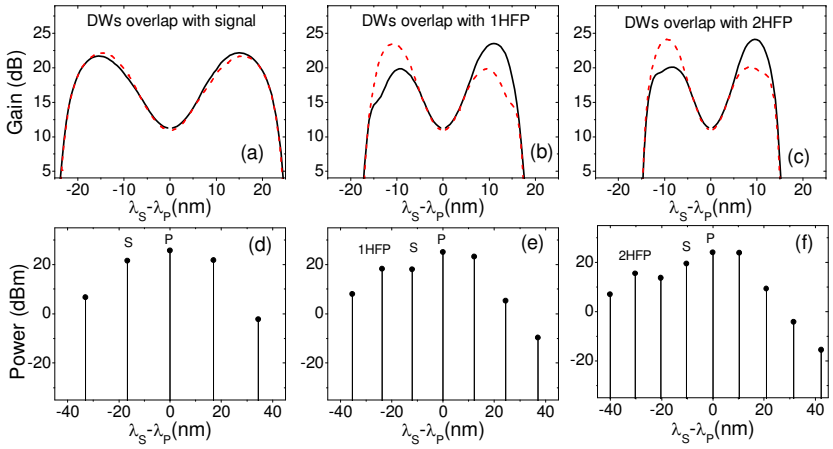

Fig. 6. Top: Simulated signal gain (solid black curve) and idler conversion efficiency (dashed red curve) spectra for three different amplifier bandwidths corresponding to overlap of the DW with the phase-matched signal wavelength on the short wavelength side (a), 1HFP (b) and 2HFP (c). Bottom: Corresponding output spectra when the signal is tuned to the phase-matched wavelength on the short wavelength side.

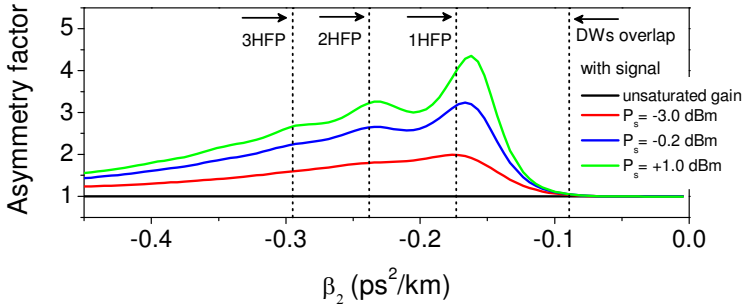

Fig. 7. Asymmetry factor (idler-to-signal output power ratio) as a function of $\beta_2(\omega_P)$ (corresponding to different amplifier bandwidths) for different signal input powers (Media 1).

#167424 - $15.00 USD Received 1 May 2012; revised 18 Jun 2012; accepted 19 Jun 2012; published 26 Jun 2012

In order to quantify the difference in power transfer to the signal and the idler (or equivalently the gain difference between two signals located symmetrically around the pump frequency) in the saturation regime, the asymmetry factor is defined as the ratio between the output idler power, $P_I(L)$, and the signal output power, $P_S(L)$

$$\text{Asymmetry factor} = \frac{P_I(L)}{P_S(L)}. \tag{6}$$

For a signal on the anti-Stokes side of the gain spectrum, the larger the asymmetry factor (≥1), the larger the spectral asymmetry. Figure 7 shows the asymmetry factor as a function of $\beta_2(\omega_P)$ for different saturation levels. In the small signal gain regime, the asymmetry factor is equal to one for all the amplifier bandwidths (corresponding to different values of $\beta_2(\omega_P)$ or equivalently $\Delta\lambda_{P0}$). The asymmetry factor becomes larger than one when the signal input power is increased to the saturation regime, indicating different energy transfers at the two sides of the spectrum.

The wavelength positions of DWs coinciding with the signal and HFPs are depicted by dashed lines in Fig. 7. The noteworthy feature in Fig. 7 is the presence of peaks when the DWs are in the vicinity of the HFPs wavelengths and local minima in-between. Overlaps of DWs with HFPs closer to the signal cause less energy transfer to the signal. In particular the overlap of the DW with 1HFP corresponds to the largest power ratio between the signal and idler. As seen in Fig. 7, the overlaps of DWs with HFPs are not exactly matched to the maximum signal-idler asymmetries. In fact, the DWs wavelengths cannot be exactly predicted from Eq. (1) as the HFPs generated during propagation through the fiber are continuously affecting the formed solitons.

Furthermore, it can be seen that the asymmetry is more pronounced for small-bandwidth amplifiers, i.e. for those with larger values of $\Delta\lambda_{P0}$, or equivalently higher absolute values of $\beta_2(\omega_P)$.

4.2 Impact of TOD

From the well-known analytical solution of the signal gain in the linear regime [5], only even orders of the dispersion contribute to the signal gain or idler conversion efficiency. It means that all the amplifiers with the same SOD value and different TOD values (i.e. dispersion slope) have the same gain spectra for small signal input powers. On the other hand, according to Eq. (1), for a fixed value of SOD the wavelength of the DW depends on the TOD and its phase matching with a fundamental soliton is only valid for nonzero values of TOD. Therefore, the effect of TOD and existence of DWs in the saturation regime can be examined by comparing the asymmetry factor of amplifiers with the same SOD (i.e. same bandwidth) but different TOD parameters. Furthermore, the value of TOD for a given coincidence between the DW wavelength and the phase matched signal, 1HFP or 2HFP can be determined from Eq. (1) according to

$$\beta_3 = \frac{3\gamma P_P - 3\beta_2 \Delta\omega_{DW}^{\ 2}}{\Delta\omega_{DW}^{\ 3}}, \tag{7}$$

where the dispersive wave coincidence with different waves can be calculated from

$$\Delta\omega_{DW} = (n+1)\Delta\omega_{PS} = (n+1)\sqrt{\frac{2\gamma P_P}{|\beta_2(\omega_P)|}}. \tag{8}$$

As earlier, the coincidence occurs at anti-Stoks side of the spectrum with the phase-matched wavelength for $n = 0$, its corresponding 1HFP for $n = 1$, and 2HFP for $n = 2$. The asymmetry factor is plotted as a function of dispersion slope for different signal input power levels in Fig. 8. In this figure the SOD is fixed and equal to –0.169 ps^2/km. This value corresponds to the dispersion at the pump wavelength of the experimental FOPA. Therefore all FOPAs obtained

#167424 - $15.00 USD Received 1 May 2012; revised 18 Jun 2012; accepted 19 Jun 2012; published 26 Jun 2012

by varying the dispersion slope in Fig. 8 have the same unsaturated gain spectrum as in Fig. 5. The asymmetry factor is equal to one for unsaturated gain, which indicates that the signal and idler have the same output powers independently of the dispersion slope magnitude, as expected.

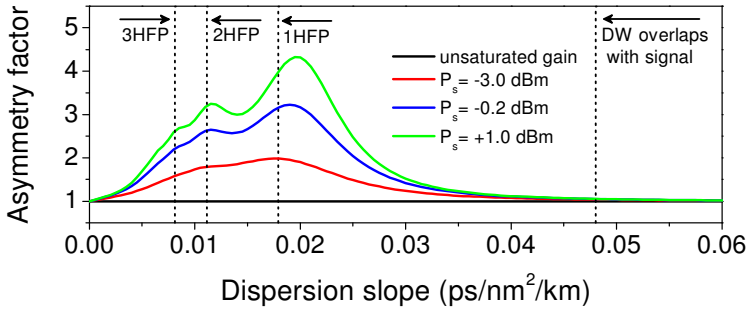

Fig. 8. Asymmetry factor (idler-to-signal output power ratio) as a function of dispersion slope for different signal input powers and for amplifiers having the same unsaturated gain spectrum.

When increasing the signal input power, some gain asymmetry is created and the asymmetry factor exhibits now different magnitudes for different dispersion slopes. As predicted by our theory, the asymmetry factor shows dominant peaks when the dispersion slope value is in the vicinity of the values calculated from Eq. (7) and corresponding to overlaps of the dispersive wave with HFPs. The most interesting point of this figure is that the maximum of the asymmetry factor corresponds to the coincidence of the DW with 1HFP, which is located beside the signal, and causes the least energy transfer to the signal in saturation, similarly to the situation shown in Fig. 7.

5. Discussion

In this section, the originality of our results and their relation to previous work is further clarified. The interpretation of an unexpected asymmetry observed in modulation instability spectra in term of interaction between solitons and dispersive wave has been proposed in [11]. Parametric amplification and modulation instability are obviously intricately related and our work builds on the original physics proposed in [11]. However, the key point of our work is the study of the effect of saturation of the parametric gain in single-pump amplifiers. To this respect, the interpretation of the observed gain asymmetry as a consequence of the interaction between dispersive waves and HFPs is novel. Inoue and Mukai [13] have reported the observation of spectral holes located around the signal wavelength in the ASE spectrum of single pump FOPAs. It is believed that the effect described in the present paper is different from the one leading to these spectral holes for a number of reasons. First, our work focuses on spectral asymmetry in the signal gain, which indeed may lead to spectral holes in strong saturation. However these holes appear only on the short wavelength side of the signal gain spectrum. In contrast, the spectral holes in the ASE spectrum observed in [13] occur for both sidebands of the gain spectrum, i.e. for both the signal and idler. No signal gain asymmetry is clearly visible in [13]. Second, in order to account for the observation in [13], a 9-wave model is implemented, including signal, pump and idler (spaced by $\Delta\nu$), as well as symmetric waves representing ASE components around those with a frequency spacing with the signal, pump and idler (Δf) smaller than that between the signal and pump (i.e. $\Delta f < \Delta\nu$). Using this model, the authors successfully reproduce the behavior of their experimental observations, i.e. the occurrence of a spectral hole in the ASE component power around the signal. In contrast, in our simulations, we need to include HFPs spaced from the pump by multiples of $\Delta\nu$ in order to account for the observed gain asymmetry. Clearly, the transfer of photons between the waves has to be different in the two cases. We highlight again that only 3 “signal” waves (signal, pump and idler) are sufficient to model the observations in [13], indicating that the presence of strong HFPs does not play a significant role in the effect described in this

#167424 - $15.00 USD Received 1 May 2012; revised 18 Jun 2012; accepted 19 Jun 2012; published 26 Jun 2012

reference, while our interpretation of the gain asymmetry in strongly saturated FOPAs requires to take a number of HFPs into account.

6. Conclusion

In conclusion, an asymmetry not expected from conventional phase matching considerations has been observed experimentally in the gain spectra of saturated single-pump FOPAs. TOD has been shown to affect the energy transfer to the signal on the different sides of the gain-saturated spectrum in FOPAs. The resulting asymmetric gain spectrum is believed to be due to the interplay between the excited HFPs in strong saturation conditions and the DWs emitted at the short-wavelength side of the spectrum. The generation of DWs is a direct consequence of the perturbation of solitons by TOD. It has furthermore been shown that dispersion plays an important role in the asymmetry feature of the saturated gain spectrum such that the asymmetry factor exhibits local maxima for particular dispersion values. The asymmetry is pronounced when the wavelength of the DWs falls on the HFPs and shows a maximum for overlap with first HFP.

#167424 - $15.00 USD Received 1 May 2012; revised 18 Jun 2012; accepted 19 Jun 2012; published 26 Jun 2012